

2025 | 470

## **X-DF-M - WinGD's new methanol engine**

Dual Fuel / Gas / Diesel

**Andrea Pastore, WinGD**

Thomas Stürm, WinGD  
Christophe Barro, WinGD  
Juan Reina Martinez, WinGD

---

This paper has been presented and published at the 31st CIMAC World Congress 2025 in Zürich, Switzerland. The CIMAC Congress is held every three years, each time in a different member country. The Congress program centres around the presentation of Technical Papers on engine research and development, application engineering on the original equipment side and engine operation and maintenance on the end-user side. The themes of the 2025 event included Digitalization & Connectivity for different applications, System Integration & Hybridization, Electrification & Fuel Cells Development, Emission Reduction Technologies, Conventional and New Fuels, Dual Fuel Engines, Lubricants, Product Development of Gas and Diesel Engines, Components & Tribology, Turbochargers, Controls & Automation, Engine Thermodynamics, Simulation Technologies as well as Basic Research & Advanced Engineering. The copyright of this paper is with CIMAC. For further information please visit <https://www.cimac.com>.

## ABSTRACT

International Marine Organization's (IMO) CO<sub>2</sub> and Greenhouse Gas (GHG) targets for 2030 and 2050 have set the challenge for Engine Designers to enhance and extend their product portfolios to include carbon neutral fuels. One of the enablers of this transition is certainly Methanol, which generates less CO<sub>2</sub> during the combustion process than distillate or residual fuels. Methanol can be produced from biomasses and renewable energy and can eventually be considered sustainable ("green" or "blue" methanol). Additionally, methanol properties (liquid at ambient temperature and pressure) make it an attractive fuel for marine applications.

This paper describes WinGD's answer to this quest with the development of the Methanol dual fuel engine technology (X-DF-M). WinGD developed a methanol injection and combustion system with simplicity and safety in focus and ensuring optimal performance, emissions and operability of the engine at the same time. Therefore, by leveraging on known solutions and commercially available components, a robust system was laid out. The WinGD methanol injection system is based on the principle of amplification of a low-pressure methanol feed by high-pressure (actuation) oil whilst injection timing and duration is controlled by the actuation oil itself. The central component of this injection system is the methanol booster unit (MBU) that is mounted on the cylinder cover. From the MBU the pressurized methanol is channeled and injected into the combustion chamber by acting on spring-controlled injection valves. Such separation of pressure amplification and injection function allows a lean and compact cylinder cover layout, key aspect for both large and medium bore engines, limited respectively by injector weight and size and space availability.

Safety during operation is ensured by double wall pipes with air ventilation or inert gas padding. Separation between methanol and system oil is guaranteed by different sealing layers, such as mechanical sealing and fluid sealing solutions, both oil and fuel itself. Similarly, safe maintenance operations and quick emptying of the system are guaranteed by a water purging approach, to benefit from the high miscibility of the two fluids and the liquid-to-liquid purging effectiveness.

To ensure high performance, efficient combustion and emission control, methanol combustion experiments in the Spray Combustion Chamber (SCC) were carried out already in an early stage and translated into the product design. The methanol injection and combustion system has been tested and optimized on a multicylinder test engine with a 520mm bore. In a second step, tests have been carried out on the new single cylinder test engine with a 920 mm bore, allowing a direct transfer of the test results to the first prototype engine, a 10X92DF-M with delivery in early 2025.

## 1 INTRODUCTION

Methanol is increasingly being recognized as a promising marine fuel due to its potential to significantly decarbonize ship operation. When burned, methanol generates lower emissions of sulfur oxides (SO<sub>x</sub>), nitrogen oxides (NO<sub>x</sub>) [1], and particulate matter compared to traditional marine fuels. As the shipping industry faces mounting pressure to reduce its environmental footprint, methanol offers a cleaner and more sustainable alternative to conventional fuels, like marine diesel oil (MDO) or heavy fuel oil (HFO).

Although emerging technologies are enabling near-zero emission production methods, the green energy supply needed for methanol production is not yet available, and it still largely depends on fossil energy sources. Nevertheless, renewable methanol, coupled with a low-emissions supply chain, can substantially lower lifecycle emissions from the shipping sector.

In comparison to other alternatives like LNG or ammonia, methanol is simpler to store and handle since it does not require cryogenic conditions. This ease of storage also leads to lower newbuilding costs for vessels using methanol as a fuel. Safety is, of course, a key concern with any fuel type, but methanol has a narrower flammability range than conventional fuels, offering certain safety advantages in specific situations. However, despite its low intrinsic toxicity, Methanol is metabolized into highly toxic compounds that can lead to blindness, coma, and life-threatening metabolic disturbances [2]. Therefore, strict safety standards and protocols must be in place to ensure the secure handling, storage, and transportation of methanol.

Methanol, as a synthetic fuel, offers a uniform chemical composition and quality. This consistency allows operators to avoid the complications of managing multiple fuel grades at various ports. Consequently, it streamlines fuel management and minimizes the necessity for complex fuel treatment systems.

With its environmental benefits, safety features, and operational ease, methanol is becoming a viable and sustainable option for the future of marine fuel.

## 2 WINGD METHANOL INJECTION SYSTEM

WinGD developed a methanol engine based on the standard diesel engine architecture. Figure 1 provides an overview of the modifications and additional components necessary to convert a pure diesel engine into a methanol dual-fuel version, the

X-DF-M. The outcome is a service-friendly and retrofittable solution.

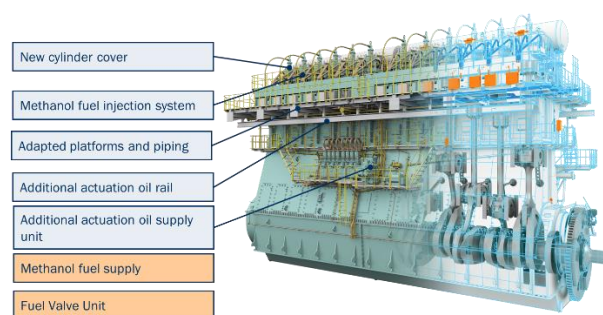


Figure 1. High-level overview of adaptations required from X- to X-DF-M engine.

### 2.1 Selection of the combustion concept

WinGD has selected a mixing-controlled combustion approach (Diesel cycle) with a diesel pilot for methanol combustion in the X-DF-M. Diffusion controlled and premixed approaches were investigated and compared to reach this conclusion. Even though, a premixed methanol combustion concept could achieve similar efficiency levels and provide a low-cost solution, the compression ratio is still constrained by autoignition, negatively affecting engine operation in diesel mode when using the same hardware. The ignition of methanol is induced by diesel pilot flames, which are supplied by the diesel injection system of the base engine in the X-DF-M engines. Several improvements were implemented to enable the diesel system to pilot the methanol flame using a minimal quantity of fuel while still meeting the 110% load requirement in pure diesel operation.

Based on the selected cycle, the layout was subsequently defined. Figure 2 illustrates the selected layout, which served as the basis for conducting CFD studies aimed at optimizing injection parameters, such as relative position and nozzle geometry. The chosen configuration features methanol injection positioned downstream of the diesel pilot in the direction of the swirl.

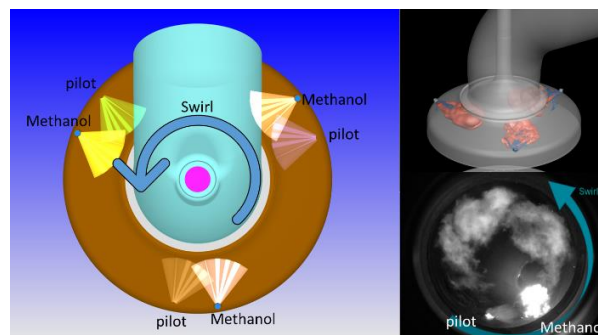


Figure 2. Pilot (diesel) and methanol injector layout.

The selected engine configuration allows for the injection of pilot fuel (Marine Diesel Oil, MDO) into the compressed air charge, creating an oxygen-rich environment that promotes combustion. The high cetane number of MDO ensures consistent and stable ignition. Although the pilot flame constitutes only a small fraction of the total power output (approximately 3-5% at high engine loads), it serves as a reliable ignition source for the injected methanol. This relatively small yet stable pilot flame provides sufficient thermal energy to initiate the combustion of the primary fuel charge. In contrast, injecting methanol upstream of the diesel pilot creates a localized oxygen-deficient environment for the pilot charge. This results in the subsequent injection of pilot fuel occurring within a methanol-oxygen mixture, which can degrade the ignitability of the pilot fuel. Additionally, this configuration presents a potential drawback: the downstream propagation of the main combustion flame towards the diesel pilot injector. This could lead to significant heat transfer to the injector component, potentially compromising its operational integrity.

## 2.2 Methanol injection system concept

The key components of the methanol injection system for the X-DF-M engine are illustrated in Figure 3. The fundamental principle of methanol injection involves amplifying a low-pressure methanol feed using high-pressure (actuation) oil. The main components of the system include:

1. Actuation oil supply unit
2. Actuation oil rail
3. Methanol booster unit (MBU)
4. Methanol injection valve

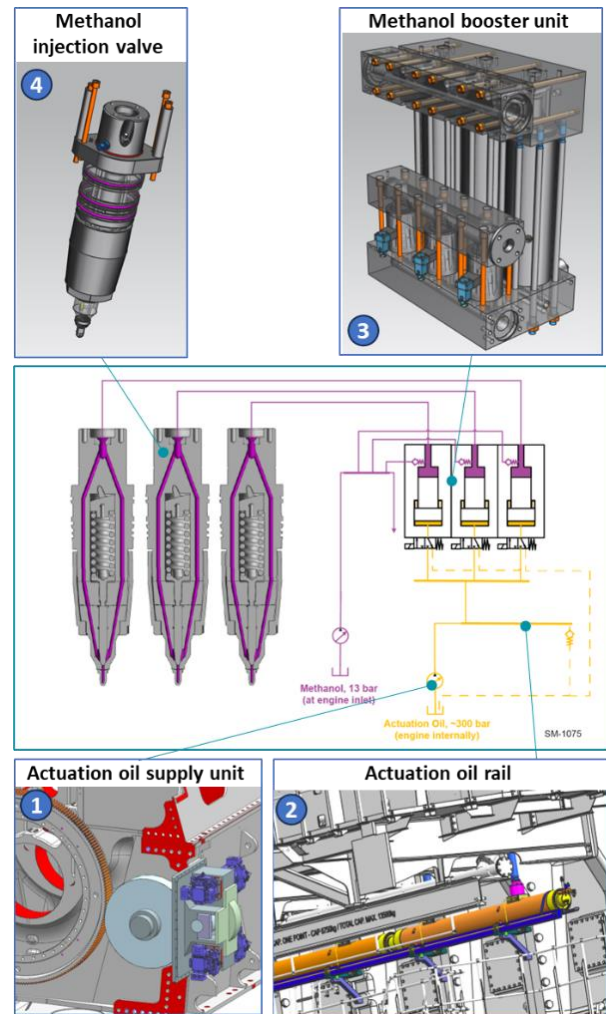


Figure 3. High level schematics of the X-DF-M fuel injection system.

### 2.2.1 Key components

This subsection offers a detailed overview of the functionality of the key components and subsystems specific to the X-DF-M engine.

#### • Actuation oil system

Hydraulic oil from the bearing lubrication system is pressurized by commercially available oil pumps that are mechanically driven by the crankshaft gear wheel (item 1 in Figure 3). The number and location of these pumps depend on the bore size and the number of cylinders in each specific engine. Figure 4 illustrates the solution for the 10X92DF-M-1.0 application in more details.



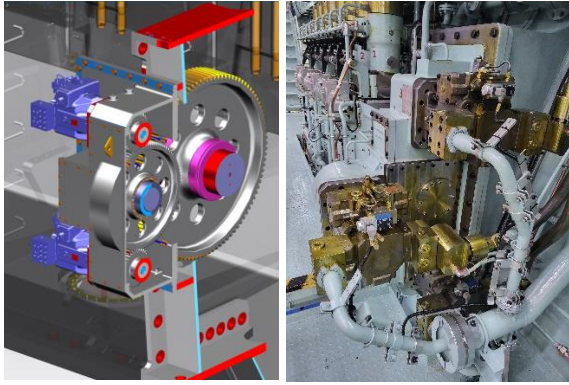


Figure 4. Actuation oil supply unit model (left) and application to 10X92DF-M-1.0 (right).

Oil pressurized to 300 bar is then stored in a dedicated actuation oil rail (item 2 in Figure 3). The volume of this rail is designed to maintain the oil pressure within a range of  $\pm 5\%$  of the target supply pressure. The high-pressure actuation oil is directed to each methanol booster unit (one per cylinder), in which the methanol pressure is amplified, and the injection controlled.

- Methanol booster unit (MBU)

The methanol booster unit (item 3 in Figure 3) comprises several components and functions, with the first being the Oil Control Valve. Here, a solenoid valve controls the opening of a spring-loaded valve when energized. Once the solenoid is activated, high-pressure actuation oil lifts the valve spindle, allowing the oil to flow to the bottom part of the MBU, where the piston of the amplifier is located.

The geometry of the spindle is meticulously designed to regulate the opening and closing velocity of the valve, which directly influences the injection characteristics and the pressure waves reflected back to the actuation oil system. When the solenoid is de-energized, the spring pushes the valve spindle back into its closed position, stopping the oil inlet. Simultaneously, passages open to allow the actuation oil to flow out of the MBU to the return connection.

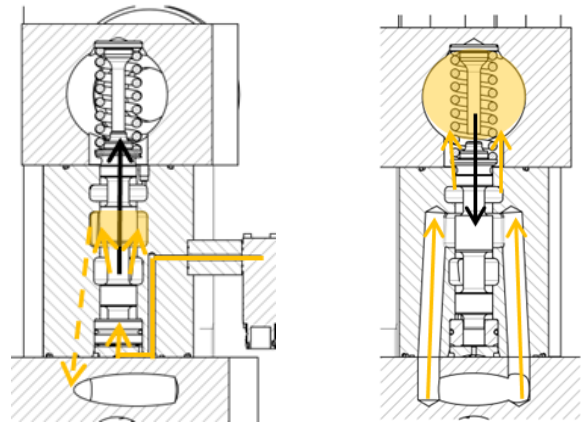


Figure 5. Functional principle of the oil control valve. Left: start of injection, right: end of injection.

The second component consists of the piston and plunger, which amplify the methanol pressure to the desired injection pressure based on their surface area ratio. The movement of the piston and plunger is monitored by a stroke sensor, as shown in Figure 6, which provides a feedback signal necessary for calculating the system's dead time to achieve the desired injection timing. Additionally, the sensor helps identify any faults within the system.

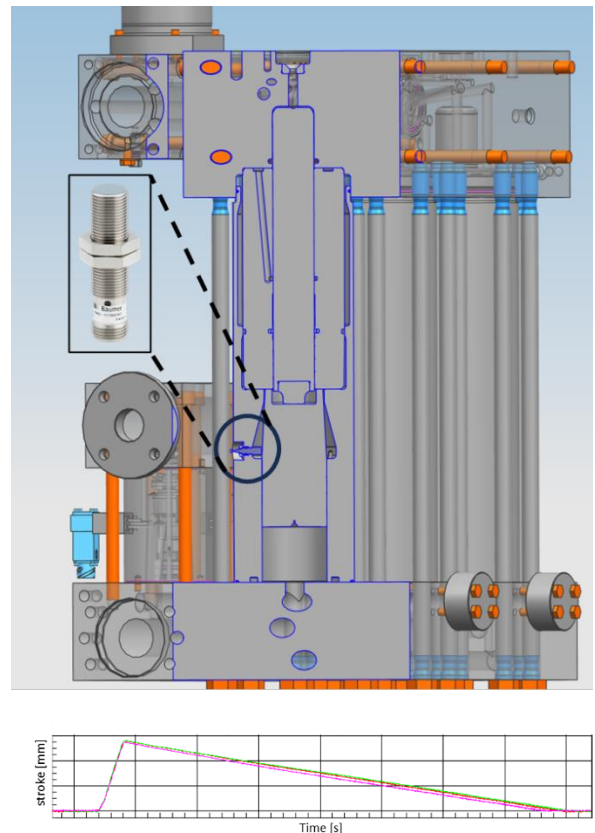


Figure 6. MBU plunger stroke sensor and signal output.

The top part of the MBU contains the methanol fuel passages and a non-return valve. During the refilling process after an injection, the plunger is pushed down by the low-pressure methanol feed. Once the solenoid is energized and the actuation oil pushes the piston-plunger assembly, the non-return valve prevents high-pressure methanol from flowing back to the feed, directing the fuel to the injection valve instead.

To ensure the separation and prevention of contamination between the system oil and methanol, several barriers are implemented, as illustrated in Figure 7. First, a low-pressure methanol barrier collects any high-pressure methanol that may leak through the plunger-cylinder clearance. Next, a second barrier with sealing oil, maintained at a higher pressure than the low-pressure methanol, ensures that oil flows into the methanol and not the other way around. Finally, a mechanical seal (rod seal) is also included to provide additional protection.

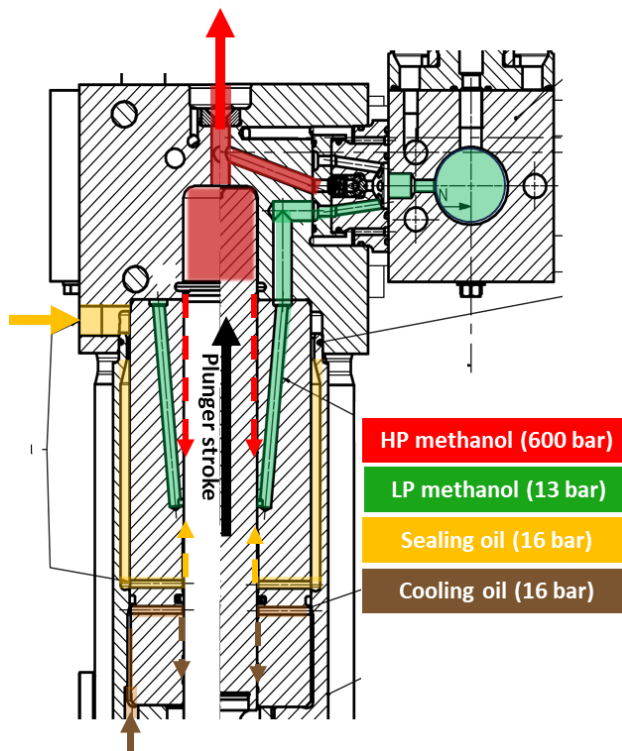


Figure 7. Overview of different media and flows within the Methanol booster unit.

- Methanol injection valve

The methanol injection valve (item 4 in Figure 3) is a simple spring-controlled nozzle; however, it requires additional safety and functional features to enable safe operations with a toxic fuel like methanol. To address this requirement, several passages and barriers are incorporated into the

methanol injection valve design, as shown in Figure 8.

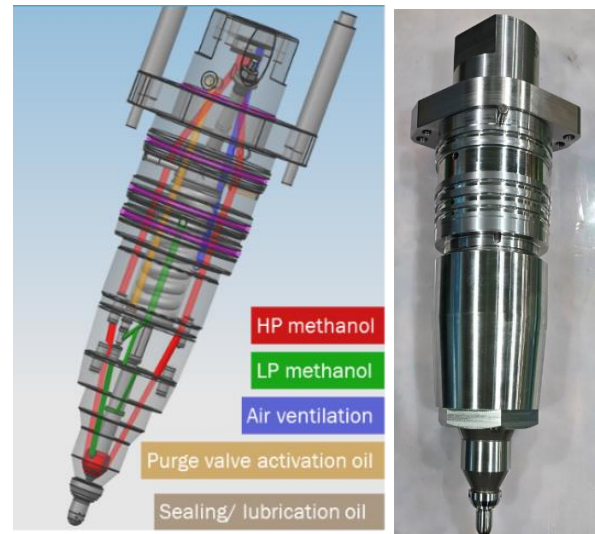


Figure 8. Methanol injection valve inner passages (left) and final manufactured X92DF-M methanol injection valve (right).

Firstly, a sealing function is provided by a low-pressure methanol barrier, similar to that in the MBU. The low-pressure methanol groove (marked in green in Figure 9) collects any leakage of high-pressure methanol through the needle clearance. Additionally, a higher-pressure sealing oil (marked in yellow in Figure 9) serves to prevent any contamination of the system oil by methanol while also lubricating the needle.

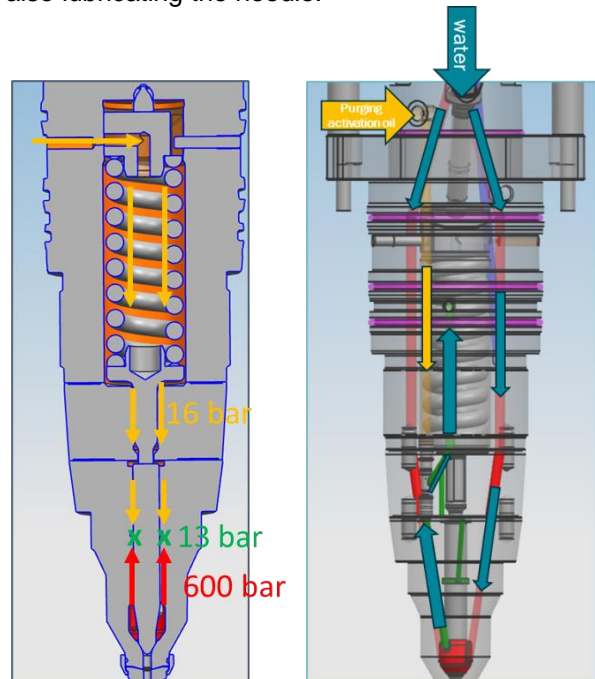


Figure 9. Methanol injection valve sealing (left) and purging principle (right).



Secondly, each injection valve is equipped with a “purge valve” that is actuated by oil. This valve facilitates the flushing of the inner channels of the injection valve with water during purging operations, ensuring safe maintenance and disassembly of the components, as shown in Figure 9.

Figure 10 shows the application of the aforementioned components in the first WinGD methanol engine (10X92DF-M-1.0).



Figure 10. Application of the methanol injection system on the first WinGD X-DF-M (10X92DF-M-1.0) engine.

### 2.3 Safety

In accordance with the IMO interim guidelines and IGC rules applicable to vessels operating on low flashpoint fuels, methanol marine engines must meet specific safety criteria. The WinGD X-DF-M methanol engines fully comply with these safety requirements.

A double-wall design is implemented for all pipes and components carrying methanol. The annular space between the inner and outer pipes serves to contain and detect any potential fuel leakage. This design protects the engine room from fuel spray (following the gas-safe machinery space concept), and the engine will trip as soon as a leakage is detected.

WinGD offers two options for the annular space: ventilation or inerting. The ventilation solution facilitates an air exchange within the annular space at a rate of 30 times per hour. A gas detector positioned upstream of the fan serves as an alarm for the presence of methanol leakage in vapor form (indicating small leakages), while liquid sensors located at the lowest points ensure the detection of larger leakages. Alternatively, the inerting solution involves a sealed and blanketed annular space filled with nitrogen and pressurized. Leakage

detection in this case is ensured through pressure rise alarms and liquid leakage sensors.

Additionally, the engine safety system ensures that any failure of the methanol system results in a trip to diesel backup mode, guaranteeing continuous and uninterrupted propulsion power availability at the shaft.

Purging and inerting of the inner passages of the methanol injection system in the X-DF-M engines are performed using water. Liquid-to-liquid purging offers several advantages over gas-to-liquid purging, and the full miscibility of water and methanol ensures an effective flushing procedure for all components as described in Chapter 3 in detail.

### 2.4 WinGD Experimental Facilities

Table 1 provides a brief overview of the test facilities used for the validation and development of the X-DF-M methanol engine introduced in the previous chapter. These are only part of the extensive testing infrastructure available in the Global 2-stroke Test Center of WinGD and CSSC [3]. The spray combustion chamber (SCC) is an optically accessible constant-volume chamber with the ability to reproduce the combustion characteristics of an engine while consuming only a fraction of the fuel. The 500 mm bore size matches that of the RTX-6, one of the test engines located at WinGD's Engine Research and Innovation Centre (ERIC) in Switzerland. The single-cylinder test engine SCE920, which is described in more detail in [4], as well as the 10-cylinder prototype engine (10X92DF-M-1.0) with a 920 mm bore, are both located at CSSC-MES Diesel Co., Ltd (CMD) in Shanghai.

Table 1. Experimental facilities with corresponding characteristics.

SCC	RTX-6	SCE92	10X92DF-M
			
Constant Volume Chamber	4-cylinder test engine	1-cylinder test engine	10-cylinder prototype engine
Bore: 500 mm	Bore: 500 mm	Bore: 920 mm	Bore: 920 mm
Stroke: -	Stroke: 2250 mm	Stroke: 3468 mm	Stroke: 3468 mm
Power: -	Power: 6496 kW	Power: 6450 kW	Power: 52000 kW
Speed: -	Speed: 105 rpm	Speed: 80 rpm	Speed: 75 rpm

## 3 ENGINE OPERATION MODES

**Methanol mode:** In this mode, both the methanol and diesel injection systems are active. The primary source of energy is provided by methanol fuel, while diesel serves to provide the pilot flame necessary for controlling the ignition of the methanol spray. Methanol operates within a load range of 10% to 100%, with diesel contributing less

than 5% of the energy at 100% load. The methanol mode can meet IMO Tier II and Tier III limits, Tier III with either low- or high-pressure SCR).

**Diesel mode:** During short diesel operations, the methanol system is kept pressurised to prevent boiling of methanol in the hottest locations (i.e., injection valve), potentially leading to corrosion of components. On the contrary, for long diesel operations, the methanol system is depressurised and purged.

**Purging mode:** In the event of, maintenance, or depressurization of the methanol system, or a leakage, purging is performed with water in two subsequent steps, as illustrated in Figure 11. First, the low-pressure feed and return pipes are purged, followed by the high-pressure methanol injection pipes and methanol injection valves. The engine volume containing methanol (including pipes and injection components) is purged 2 to 3 times to ensure the complete removal of methanol. At the end of the purging process, the system can be manually drained of water before maintenance operations.

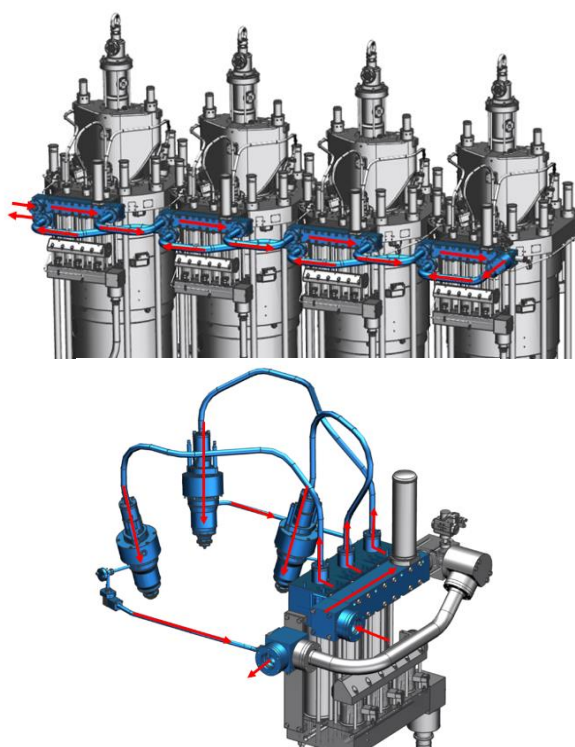


Figure 11. Water purging principle of the X-DF-M engine methanol injection system. Top: low-pressure system purging, bottom: high-pressure system purging.

This unique method for purging the methanol system has been tested on both the SCE920 and the 10X92DF-M-1.0 engines. The purging effectiveness was measured by means of two

methodologies. For the SCE920, samples were collected at the fuel return engine connection and analysed after introducing increasing amounts of water into the methanol injection system — specifically, one, two, and three times the volume of the pipes and components containing methanol. As shown in Table 2, safe conditions were achieved after purging with just twice the volume.

Table 2. Methanol concentration from the samples taken at the SCE920 after each purging sequence.

Volume purged [times]	Methanol concentration [%]
1X	3.5
2X	0.01
3X	0.03

On the 10X92DF-M-1.0, a conductivity sensor was installed downstream of the engine outlet connection, and purging was performed based on a time-based approach, consisting of three purge cycles, each lasting two minutes with a pause in between.

Although the conductivity of pure water and methanol is only slightly different, the sensor successfully detected the change, signalling the completion of the purging process.

**Leakage and functional check:** During commissioning, after maintenance, or following a prolonged standstill of the methanol system, a leakage and functional test is conducted as standard procedure. This operation is also performed using water, which provides an easy and visual method for detecting leakages compared to inert gas leakage checks. Similar to the purging operation, the process begins with pressurizing the low-pressure system, followed by a second step in which the high-pressure components and connections are checked. Inspection plugs are removed to visually detect and localize any potential leakages, eliminating the need for cylinder isolation valves and additional sensors.

## 4 INJECTION SYSTEM SIMULATION

### 4.1 1-D hydraulic simulations

In the early stages of the X-DF-M development, a 1-D hydraulic simulation model was established in Simulink to design the methanol injection system. This approach proved invaluable in selecting the optimal injection concept and determining appropriate dimensions. For instance, the advantages and disadvantages of an injector with an integrated pressure amplifier were compared to the MBU concept (see chapter 2.2.1). The simulation results indicated no significant



differences in injection shape. However, the design analysis highlighted clear advantages of the MBU concept, particularly in its simplified fuel supply system and user-friendly injector, which facilitates easy maintenance.

Once the concept was established, a one-cylinder model enabled rapid iteration of various parameters. With each iteration taking only 20 seconds, all components of the injection system could be efficiently fine-tuned and optimized, including pipe sizes and the dimensions of the MBU and injector parts.

An example of an optimization loop can be illustrated with the actuation oil pipe. A smaller pipe diameter facilitates easier arrangement, as it is more flexible and experiences less alternating stress due to relative movements between connected components during engine operation. Additionally, manufacturing and cost considerations favor a smaller pipe. However, from a hydraulic perspective, the benefits trend in the opposite direction. A reduced flow cross section results in higher flow speeds and, consequently, increased acceleration forces. These high acceleration forces lead to significant pressure pulsations, which can stress the pipe and its supports. To address these challenges, it is essential to conduct a finite element analysis (FEA) of the pipes and its supports to evaluate these limits. This analysis provides valuable feedback on the hydraulic layout, creating an iterative process that integrates hydraulic simulation, geometric design, and FEA results.

Another example is the dimensioning of the plunger high-pressure seal, which functions as a long, narrow gap that throttles the leakage flow. The thinner and longer the clearance gap, the lower the leakage flow; however, the effect of gap height on leakage flow goes with a cubic law. While minimizing the clearance height is desirable and requires no additional space, other limiting factors must be considered, such as thermal expansion, which can lead to seizing, as well as manufacturability constraints.

The resulting clearance flow is integrated into the simulation model. In addition to the loss of volumetric efficiency, it is evident that the backflow from the plunger leakage disrupts the low-pressure fuel supply system. To maintain pressure spikes from the leakage flow within  $\pm 3\text{bar}$ , the plunger clearance length had to be designed in a way that it allows a simple and still fatigue resistant pipe system due to low vibrations.

A further consideration was the dimension of the internal leakage flow bores. They had to be

sufficiently large to prevent pressure spikes overcome the sealing oil pressure level. This feedback from the hydraulic simulation enabled the design of a system with a low sealing oil pressure of only 16 bar, ultimately resulting in very low sealing oil consumption.

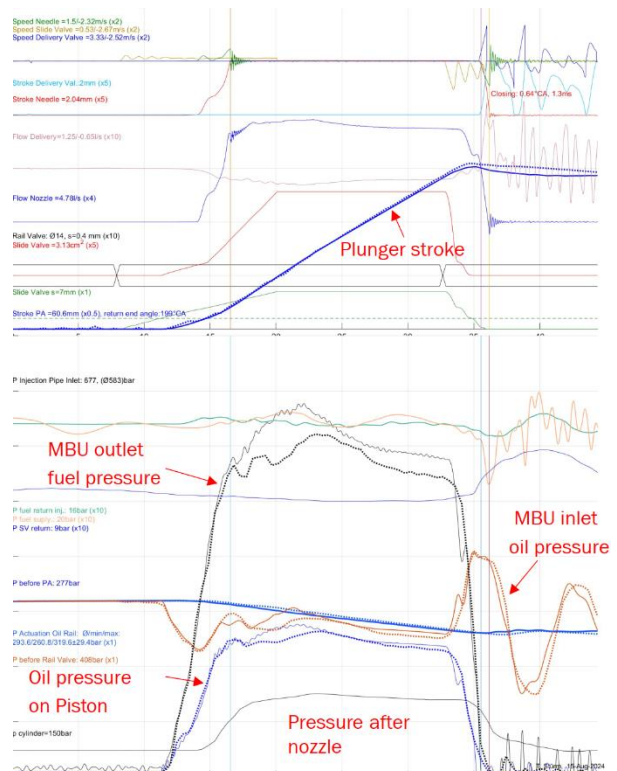


Figure 12. Hydraulic simulation of the X-DF-M injection system (single injection). The continuous lines represent the simulation result, the dashed lines represent the experimental data.

In the next phase, the model was extended to a multi-cylinder configuration to analyze the interactions between the cylinders. This extension allowed refining the actuation oil rail and the fuel supply system design. Additionally, the sealing oil and low-pressure oil return pipe systems were simulated and designed accordingly.

Beyond component dimensions, the simulation also provided insights into sealing and actuation oil consumption, ensuring that acceptable values could be achieved.

The system simulation initially facilitated the layout of the methanol injection system and provided the necessary parameters for the detailed design of the injection components. Ultimately, the validation of the hydraulic performance on the hydraulic rig (Figure 12 dash lines) led to the calibration of the model and optimization of the components, all in time for the testing of the X-DF-M prototype.

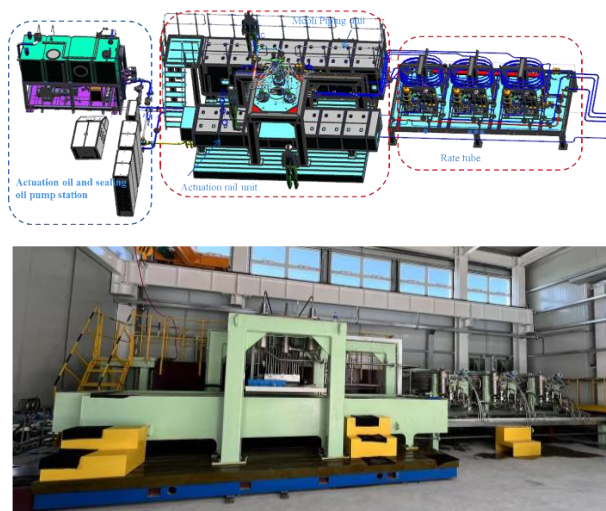


Figure 13. WinGD methanol hydraulic rig test facility in Lingang, Shanghai.

## 4.2 CFD simulations

Leading-edge computational fluid dynamics (CFD) methodologies were deployed to advance the development of the X-DF-M engine platform. The numerical framework incorporated classical well-known RANS/RNG/Lagrangian modeling coupled with sophisticated detailed chemistry combustion approaches. An innovative approach to unify the chemical mechanism was developed, enabling simultaneous simulation of MDO and methanol combustion through refined kinetic models centered on strategically selected surrogate molecules (example given in Figure 14). Model validation was performed against experimental data obtained from the Spray Combustion Chamber.

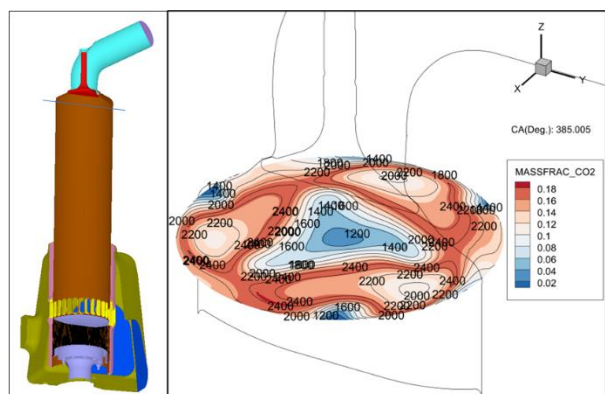


Figure 14. CFD study air exploitation for spray pattern optimization with methanol diffusive combustion on a X92-DF-M-1.0 model, 50% load. Iso temperature lines (°K), CO<sub>2</sub> mass fraction contour map.

The parametric investigation explored the optimization of methanol injection characteristics, like injection pressure variations, nozzle geometry configurations, and spray pattern dynamics. These

findings are adequately documented in previous publications [5].

Subsequent investigations focused on characterizing the internal flow dynamics within the methanol injection valve utilizing a hybrid RANS/DDES (Delayed Detached Eddy Simulation) methodology. This advanced numerical approach enabled high-fidelity simulation of steady-state flow characteristics throughout the intricate internal geometry of the injector assembly. The CFD results were used as a robust validation framework for one-dimensional flow simulations, particularly concerning discharge coefficients and pressure loss characteristics. The observed 10% discrepancy between one-dimensional and three-dimensional CFD simulations (Figure 15) stems from inherent differences in computational domain definitions - the 1D approach encompassing the complete flow path while the 3D-CFD methodology necessarily employs a truncated geometric representation. Despite this systematic variance, the comparative analysis, focused on parametric trend evaluation, demonstrated robust correlation between numerical predictions and experimental measurements, thereby validating the fundamental flow physics captured by both computational methodologies.

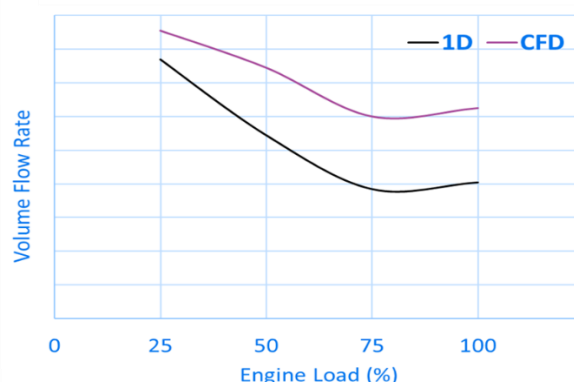


Figure 15. Comparison CFD-1D simulation of methanol volume flow rate through the nozzle holes.

Multiphase flow modeling incorporating Volume of Fluid (VOF) methodology coupled with the Schnerr-Sauer cavitation model was integrated into this framework. The resulting computational approach represents a significant advancement in cavitating flow prediction, enabling good assessment of cavitation phenomena and associated risks. Numerical simulations revealed the absence of cavitation in the needle seat region, while identifying localized cavitation inception zones at the nozzle hole entries, with maximum intensity observed in the uppermost orifice.

The predicted cavitation structures and their spatial distribution were deemed non-critical from a design perspective, considering that the simulated geometry represented nominal dimensions without accounting for post-manufacturing surface finishing effects, which typically result in enhanced edge smoothing. Mitigation strategies including increasing the edge smoothing and convergent nozzle profiles to suppress cavitation phenomena have been already anticipated.

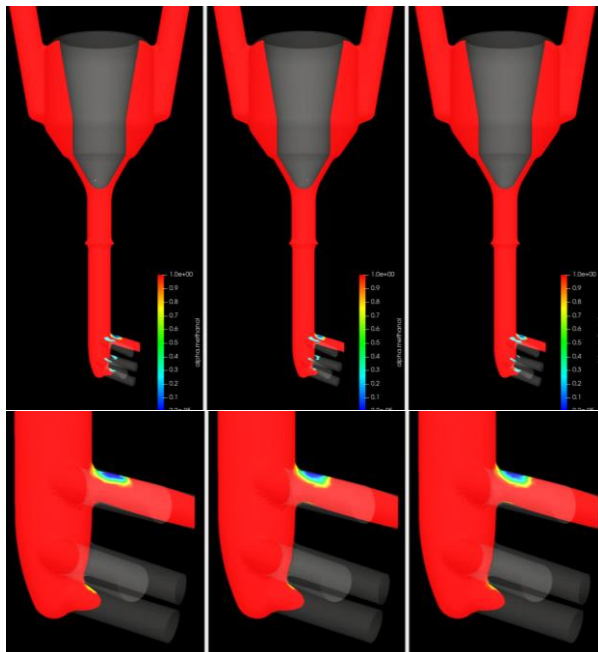


Figure 16. CFD results of pressure in the inner methanol injection valve regions 50%, 75% and 100% load from left to right. Top: needle seat and sac volume, bottom: details of nozzle holes.

## 5 COMBUSTION PROCESS DEVELOPMENT APPROACH

The following section summarizes and validates the WinGD development approach, including a comparison between the RTX-6 test engine results and those from the SCC, which served as the initial data source for model calibration. The last section presents the results achieved on the 10X92DF-M-1.0.

### 5.1 Combustion process development approach

Figure 17 outlines a hierarchical simulation toolbox for the development and prediction of the combustion system behaviour.

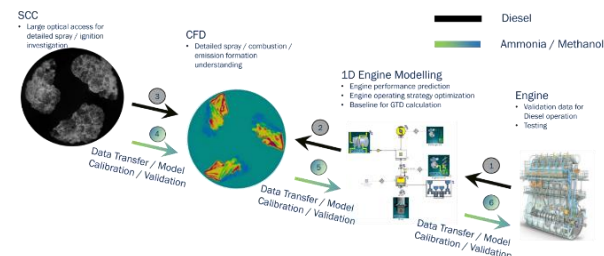


Figure 17. Overview of WinGD's future fuel development approach [5].

This development strategy is crucial since the sub system layouts, which depend on performance prediction need to be done long before a test engine exists. In addition, once a test engine is available, the performance and emission prediction need to be extended to the entire portfolio. The toolbox combines a 1-D engine model using GT-POWER with predictive combustion and emission sub-model. For model validation, simulation results are compared to experimental data, first using conventional diesel fuels, then extending to methanol/ammonia dual-fuel combustion. The successful validation led to the creation of a parametric model for a dual-fuel combustion system, which was validated and used to forecast performance for test engines. The results help optimize the design and development process for future production engines, improving efficiency and reducing development time. This toolbox is explained in more detail in [5].

### 5.2 Validation of development approach

Figure 18 shows a comparison of the heat release rate from the SCC and the test engine RTX-6 at 25% of rated power in methanol operation, with one out of three injector pairs active to match the conditions of the SCC. The heat release rates exhibit a very similar shape and combustion characteristic, with a methanol-typical fast late combustion phase. This confirms the relevance of experimental data obtained on the SCC for actual engine operation and thus demonstrates the robustness of the development process shown in Figure 17. Its early availability and flexibility to switch between fuels without major conversion work make the SCC a highly valuable element of this development approach. Moreover, the optical access facilitates the establishment of much deeper insight into the fundamental processes involved and how these contribute to the overall behaviour than any engine experiments can ever



provide.

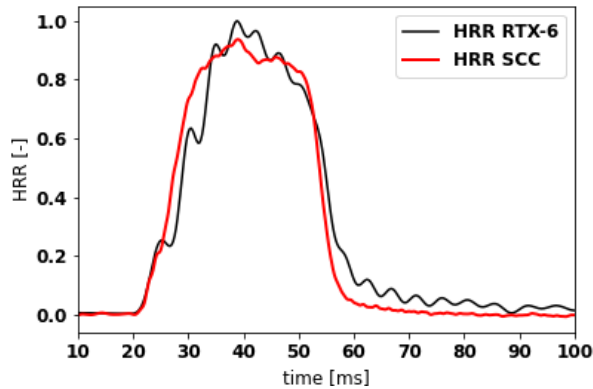


Figure 18. Comparison of heat release rate of SCC (red) and RTX-6 (black) in methanol operation.

Figure 19 shows a comparison of the RTX-6 test engine and the GT-Power model with its predictive combustion model. The figure illustrates the engine operating at 25% power in methanol operation with three different injection strategies, including a variation in fuel pressure (blue vs. black) and a variation in the number of active injector pairs (2, red vs. 1, black). The heat release model can accurately predict the differences in combustion behaviour with these variations in operational strategy.

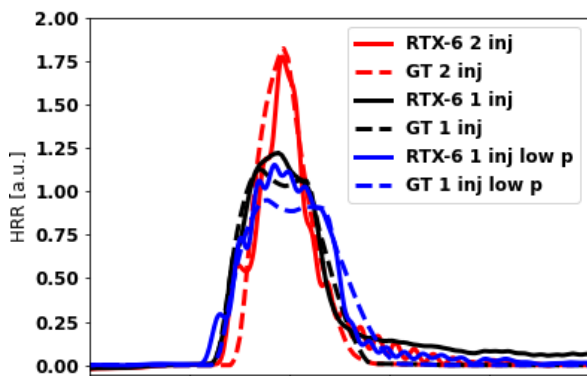


Figure 19. Comparison of heat release rates between RTX-6 experimental results (solid) and GT-Power simulation (dashed) in methanol operation using 3 different injection strategies: One injector pair active with varying fuel pressure (black, high fuel pressure, blue low fuel pressure) and two injector pairs active (red) at 25% rated engine power.

## 6 ENGINE TEST RESULTS

### 6.1 Combustion analysis of test engines

In 2-stroke marine engines with a central exhaust valve and multiple circumferentially located fuel injectors, one of the challenging situations for all models is spray-to-spray interaction during longer injection durations with all injector pairs active. This

typically occurs at higher engine loads. Figure 20 shows a comparison of heat release rates from three different engines, each operating at 100% rated power (top: RTX-6, bottom: SCE920). Both test engines are operated in both diesel (black) and methanol mode (blue). The characteristics of the heat release rates show similar behaviour, irrespective of bore size, rating, or number of cylinders. The injection duration is always longer than the corresponding peak of the heat release rate. This indicates significant spray-to-spray interaction, where not only air is entrained into a spray, but also combustion products from the upstream spray. The combustion process can be divided into three phases: (1) a free spray phase, up until the peak of the heat release rate; (2) a phase of spray-to-spray interaction, which ends at the next visible hump in the heat release rate, typically marking the hydraulic end of injection; and (3) late-phase combustion, where air-fuel mixing deteriorates due to increasing combustion products in the entrained charge and the fast dissipation of spray-induced turbulence.

In the case of the SCE920, a small initial bump from the pilot fuel combustion is visible. In contrast, for the RTX-6, the pilot injection timing is closer to the start of the main injection, making it less noticeable as a separate combustion phase. Apart from the pilot combustion phase, diesel combustion can be characterized using the same criteria. For the RTX-6 (top), late-phase combustion can be visibly separated from the second phase. This is not possible for the SCE920, as the combustion rate reduction in the second and third phases is on a similar level. Even though the reduction in heat release rate in phase 2 is significant in both methanol cases, the late-phase combustion speed (phase 3) remains considerably faster than in the corresponding diesel cases. The reason for this difference in combustion behavior between methanol and diesel lies in the fuel composition of methanol. The oxygen content in methanol reduces the stoichiometric air-to-fuel ratio and enables faster mixing to a similar stoichiometric level.



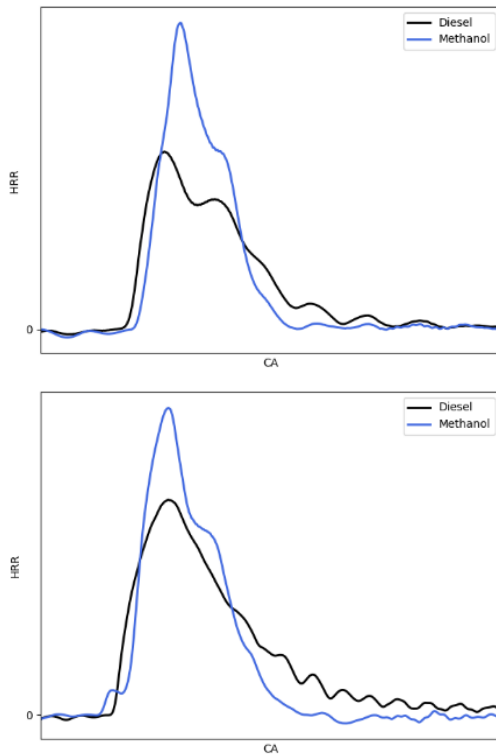


Figure 20. Comparison of experimental heat release rates from RTX-6 (top) and SCE920 (bottom) with methanol (blue) versus diesel (black) at 100 % of rated engine power.

## 6.2 Test results of the 10X92DF-M-1.0 engine

The test campaign of the 10X92DF-M-1.0 engine took place in December 2024 and early January 2025. The test included, after a first commissioning and running-in phase, base curves in diesel mode, base curves in methanol mode, test of transfers from diesel to methanol and vice versa, component temperature measurements, thermal management test (EWG testing), nozzle variation test, methanol operation optimisations (i.e., pilot consumption optimisation) and LP-SCR test with methanol. Some relevant results are reported in this section.

### 6.2.1 Combustion analysis

The following section presents the heat release rates of the 10X92DF-M-1.0 in both diesel and methanol modes. The combustion behavior is compared to the corresponding behavior of the test engines. Additionally, the GT Power model has been applied with the relevant inputs (e.g. actual injection durations), and the results are displayed accordingly. Figure 21 shows the aforementioned heat release rates for four different load points: 100%, 75%, 50%, and 25% (from top to bottom). The 100% load point demonstrates very similar combustion behavior in both diesel and methanol modes as the test engines, particularly the SCE920. The methanol combustion process again

shows a significant reduction in heat release after its peak. In comparison to diesel combustion, the late-phase combustion is considerably faster. As the load decreases, the heat release reduction due to spray interaction diminishes. This is because the shorter injection duration, as a consequence of the reduced load, results in less interaction between the sprays. The late-phase combustion remains faster than the corresponding diesel case across the entire load range. The shorter combustion duration leads to an improvement in engine efficiency, which will be discussed in more detail later. The displayed model results show excellent agreement with the measurements with negligible deviation of the peak HRR at low loads. The applied injection system and strategy facilitated favorable methanol combustion behavior, which can be modeled with a high level of accuracy. This suggests that the key combustion processes have been well understood, allowing for efficient model-based extrapolation to other bore sizes.

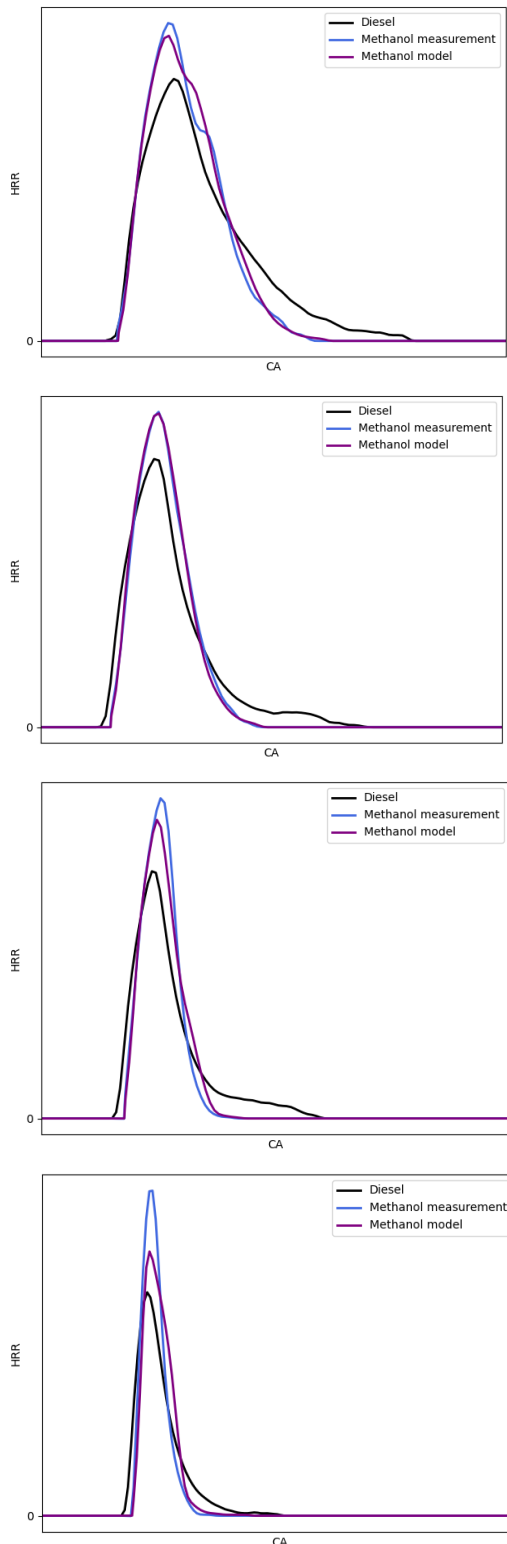


Figure 21. Comparison of heat release rates from 10X92DF-M-1.0: Experimental diesel (black), experimental methanol (blue), model methanol (purple) under 100%, 75%, 50% and 25% engine load (from top to bottom).

### 6.2.2 Energy consumption

Figure 22 shows the energy consumption in diesel and methanol mode, as measured during the shop test (FAT) of the 10X92DF-M-1.0 engine.

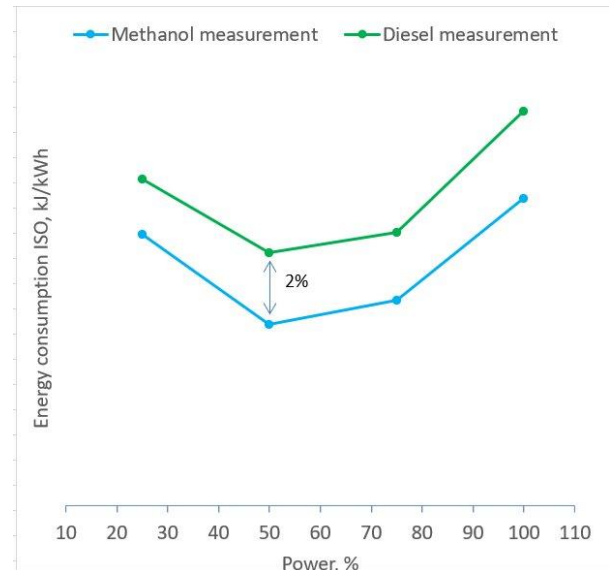


Figure 22. Comparison of energy consumption of 10X92DF-M-1.0 in diesel (green) and in methanol mode (blue).

The results are matching very well the expectations and performance guarantees. The origin of the difference between the two consumption curves can be attributed to the distinct combustion behaviour, as previously described. In general, a 1.5%-2.5% lower fuel consumption in methanol mode compared to diesel mode was confirmed through the entire load range.

### 6.2.3 Emissions

Another key difference between diesel and methanol combustion is the formation of NO<sub>x</sub>. To comply with Tier II standards, the load-specific NO<sub>x</sub> emissions must not exceed those observed in diesel mode. The high latent heat of vaporization of methanol leads to a reduction in combustion temperature compared to diesel and the lower combustion temperature helps maintain NO<sub>x</sub> levels that are similar to, or lower, than those in diesel combustion, even with shorter combustion duration, thereby improving energy consumption. In the end, there is no significant difference between engine-out NO<sub>x</sub> emissions in Tier II and Tier III between the two fuels as this was the engine tuning target, as depicted in Figure 23. Since NO<sub>x</sub> emissions are typically in trade-off with energy consumption, the engine is tuned such as the NO<sub>x</sub> emissions always stay below diesel mode level to comply with Tier II/III regulations. In higher engine load, this trade-off behaviour is impacted by other factors as peak pressure and component

temperature limitations. Under similar peak pressure conditions, NO<sub>x</sub> in methanol mode is 15-20% lower as in diesel mode.

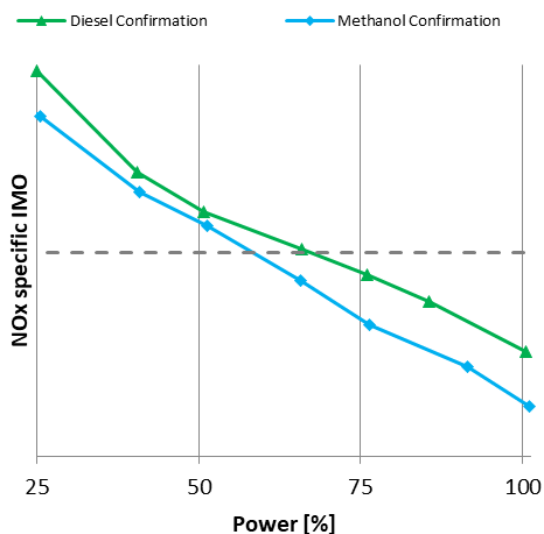


Figure 23. NO<sub>x</sub> emissions of 10X92DF-M-1.0 in diesel (green) and in methanol mode (blue).

NO<sub>x</sub> reduction for Tier III compliance is achieved through selective catalytic reduction (SCR) in both fuel modes.

Measurements of formaldehyde (CH<sub>2</sub>O) and hydrogen cyanide (HCN) were also performed during the test phase. CH<sub>2</sub>O was measured to be below 15ppm and HCN below 10 ppm in both Tier II and Tier III mode.

#### 6.2.4 Pilot consumption

Figure 24 shows the pilot energy consumption in methanol mode in relation to the corresponding energy consumption in diesel mode, along with the associated guarantee (GTD) and tolerance. The pilot energy consumption is mainly limited by the minimum possible amount of the diesel injection system. The ignition of methanol is very stable and not highly sensitive to the pilot injection timing.

The results are perfectly in line with expectations, guaranteed performance and project targets.

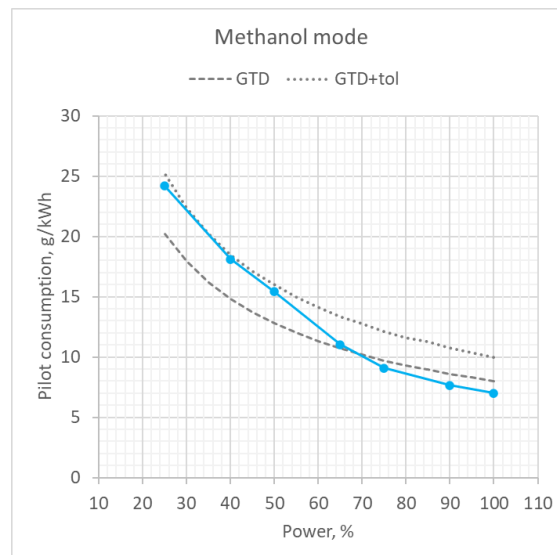


Figure 24. Pilot energy consumption of 10X92DF-M-1.0 in methanol mode against GTD data.

#### 6.2.5 Fuel transfer

Fuel transfer from diesel to methanol (and vice versa) and methanol trips were tested during the test campaign with satisfactory results. Figure 25 gives an example of a diesel to methanol transfer, executed within less than a minute at 75% engine load, followed by a methanol trip which was completed within one engine cycle. During the trip there was no noticeable impact on engine speed and load, confirming the ability of the engine of switching to back-up (diesel) mode within one engine revolution and without significant fluctuation of engine power.

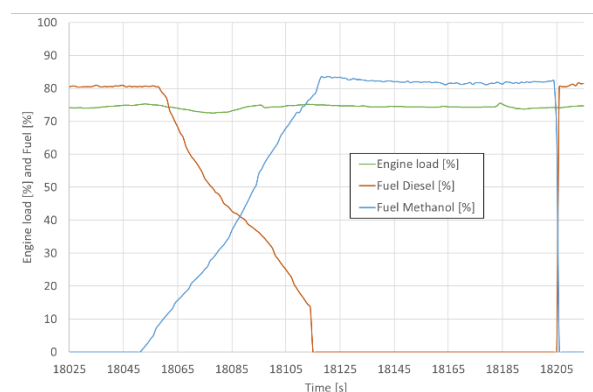


Figure 25. diesel to methanol transfer followed by a methanol trip.

#### 6.3 Factory Acceptance Test (FAT)

The final verifications on the engine with the project stakeholders for commercial application roll-out were the Factory Acceptance Test (FAT) carried out in the presence of the customer and the Type Approval Test (TAT) certification, which is

conducted in the presence of all Classification Societies.

The FAT of the first of four 10X92DF-M-1.0 engines for 16,000 TEU container carriers (end customer COSCO) was held from 13-17<sup>th</sup> of January 2025 at engine builder CSSC-MES Diesel Co., Ltd. (CMD), in Shanghai, China.

The engine is CMCR rated at a power output of 52000 kW at 75 rpm, with BMEP of 18 bar. The engine has a standard tuning, configuration and with a clockwise direction of rotation. The engine tuning has been optimised for Tier 2 diesel, Tier 2 methanol and Tier 3 in both modes with LP-SCR. The surge margin on diesel mode 100% load is 14.8% and on methanol mode 100% load is 16.9%.

The FAT included the following 5 sections:

- 1 Safety Tests
- 2 WiCE Functional Tests
- 3 Load Tests
- 4 Speed Control (Governor) Test
- 5 Lowest Steady Speed Test

At the end of this sequence of testing, which were successfully executed, noise emission, vibrations, and parts inspections were carried out. The noise level at all measured points was below 110 db(A), vibrations at all measurement points was below the limits and all inspected parts were found in good conditions.

#### 6.4 Type Approval Test (TAT)

After the successful FAT, the Type Approval Test (TAT) was carried out as an important final verification step where the Engine is required to fulfil all the regulatory requirements from IMO as far as safety is concerned. The Type approval of an Engine essentially consists of drawing and specifications approval, conformity of production, approval of type testing programme, type testing of engines (TAT), review of the obtained results, and the issuance of the Type Approval Certificate (TAC).

The TAT comprised of a comprehensive set of safety and functional tests in diesel and methanol modes, the safety and functional integration of WiCE engine control system to the engine, emergency operation tests, load tests and a final inspection of the main components after all the testing was completed, carried out according to the International Association of Classification Societies IACS URM781 (Unified Requirements). The TAT for the 10X92DF-M-1.0 engine was witnessed by eight of the major Classification Societies and was held from 21-24<sup>th</sup> of January 2025, at the CMD facility.

After the four-day intense testing phase, the 10-cylinder X92DF-M-1.0 engine came through positively, performing as desired in all the sections of testing, paving the way for a successful completion of the TAT certification of the first Methanol engine of the XDF-M portfolio. The TAT was passed without any comments or official remarks (for modifications or improvements).

On a final note, Figure 26 is the Type Approval Certificate from China Classification Society (CCS), the main Classification Society in charge of the first Methanol project.

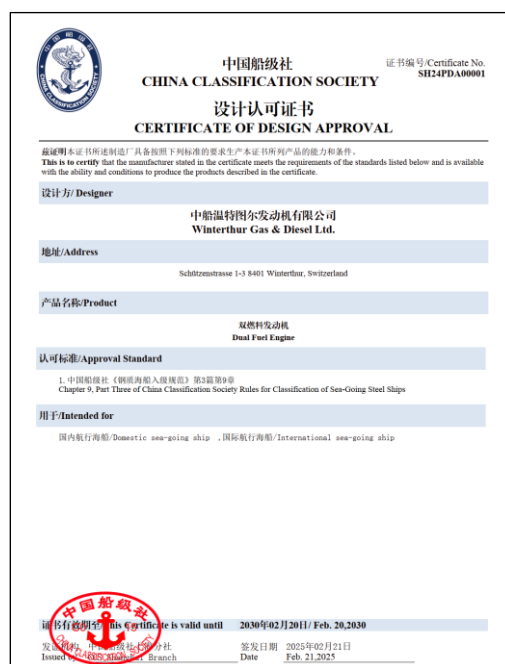


Figure 26. X-DF-M Type Approval Certificate from China Classification Society (CCS).

## 7 CONCLUSIONS

The 10X92DF-M-1.0 successfully passed its factory acceptance test (FAT) and type-approval-test (TAT), meeting the requirements for Tier 2 and Tier 3 operation. With fuel consumption figures fully within expectations, the 10X92DF-M-1.0 became the first commercial WinGD X-DF-M engine capable of operating with methanol as a fuel.

Furthermore, the approval tests were conducted on the first engine of the series, rather than on a later model as was done in previous projects. As a result, the full approval of the X-DF-M engine by the classification societies has demonstrated that the methanol system concept and design selection, along with the development iterations, safety features, control system integration, and validation process, have successfully facilitated a first-time-right introduction of this technology.



To reach this target and since test engines of the required size were not available at the beginning of the development, an alternative development approach had to be applied. The previous figures validate the applied approach, and the successful completion of the TAT demonstrates its effectiveness.

Based on the successful introduction of the first prototype, the roll-out of the system is now taking place according to Figure 27, ranging from the smallest to the largest WinGD portfolio engine bore size.

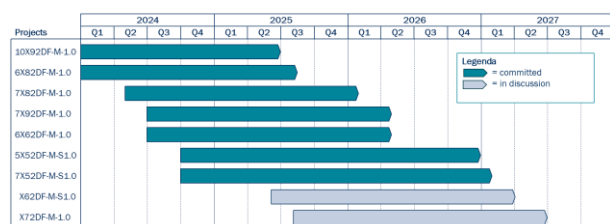


Figure 27. X-DF-M rollout to WinGD portfolio engines.

## 8 DEFINITIONS, ACRONYMS, ABBREVIATIONS

**AMS:** Alarm monitoring system

**BMEP:** Brake mean effective pressure

**CMD:** CSSC MES Diesel Co. Ltd.

**CMCR:** Contracted maximum continuous rating

**EWG:** Exhaust waste gate

**FAT:** Factory Acceptance Test

**FVU:** Fuel valve unit

**GTD:** General technical data for WinGD 2-stroke engines

**IGF:** International Code of Safety for Ships Using Gases or Other Low flashpoint Fuels

**IMO:** International Marine Organization

**LNG:** Liquefied Natural Gas

**MBU:** Methanol Booster Unit

**SCC:** Spray Combustion Chamber

**SCE920:** single cylinder engine 920 mm bore size

**TAC:** Type approval certificate

**TAT:** Type Approval Test

**TC:** Turbo charger

**WiCe:** WinGD integrated Control Electronics

## 9 ACKNOWLEDGEMENTS

The authors would like to deeply thank all the WinGD Switzerland and WinGD China members of the Methanol Technology Team who strongly contributed to the development, design, review and test preparation and test execution at the Global Test Center facilities.

Special thanks also to CSSC MES Diesel Co. Ltd. (CMD) for the invaluable support and collaboration which led to a successful test campaign of the first X-DF-M prototype and eventual passing of the FAT and TAT of this engine type.

## 10 REFERENCES AND BIBLIOGRAPHY

[1] Verhelst S., Turner J., Sileghem L, Vancoillie J., 2019. Methanol as a fuel for internal combustion engines. *Progress in Energy and Combustion Science*.

[2] World Health organisation, 2017. Methanol poisoning outbreaks.

[3] Hensel, S., Gerber, P., Karrer, I., Schleppe, T., Schmidle, M., Süess, P., von Rotz, B., Bo, L. 2023. Preparing for future demands - the CSSC Global 2-stroke Test Center. *CIMAC*.

[4] Spahni, M., Zhou, X. Y. 2025. SCE920 - Key enabler for the roll-out of validated new technologies to largest engine sizes. *CIMAC*

[5] von Rotz B., Süess P., Bohnenblust M., Barro, C., Seddik O., Reina Martinez, J., Schirru, A., Schmid, A., Weisser G. 2024. Experimental investigations and simulation validation regarding future fuel combustion systems of low-speed two-stroke engines using WinGD's spray and combustion chamber. *8th Rostock Large Engine Symposium*, Rostock, pp. 16-35.